The microwave spectra of the conformers of n-butyl nitrate

Susanna Stephens, Eléonore Antonelli, Alexander Seys, Ha Vinh Lam Nguyen, Stewart Novick, S.A. Cooke, Thomas Blake

The Microwave Spectra of the Conformers of *n*-Butyl Nitrate

Susanna L. Stephens,[a] Eléonore Antonelli,[b] Alexander B. Seys,[a] Ha Vinh Lam Nguyen,[b,c]
Stewart E. Novick,[a] S. A. Cooke,[d] Thomas A. Blake[e*]

[a]*Department of Chemistry, Wesleyan University, Middletown, CT, USA*

[b]*Univ Paris Est Creteil and Université Paris Cité, CNRS, LISA, F-94010 Créteil, France*

[c]*Institut Universitaire de France (IUF), F-75231 Paris Cedex 05, France*

[d]*Natural and Social Science, Purchase College SUNY, Purchase, NY, USA*

[e]*Chemical Physics and Analysis, Pacific Northwest National Laboratory, Richland, WA, USA.*

Number of text pages: 23

Number of Tables: 6

Number of Figures: 5

*Corresponding author: Thomas A. Blake

Abstract

The microwave spectrum of *n*-butyl nitrate was recorded in the 5 to 20 GHz frequency range using broadband chirp and narrowband pulse excitation molecular jet Fourier transform microwave spectrometers. A quantum chemistry structural analysis yielded thirteen stable conformers. Among them, the five most energetically stable conformers were observed in the experimental spectrum. The most stable conformer features a butyl chain with an *anti-gauche-anti* conformation (*AGA*) where the γ-carbon atom is about 64° out of the nitrate plane. For this conformer, spectra of all ^{13}C and ^{15}N minor isotopologues could be measured. The conformer with a straight butyl chain (*AAA*), and three other conformers (*GAA*, *GGA*, and *AGG*) were also observed. Accurate rotational constants, centrifugal distortion constants, and ^{14}N nuclear quadrupole coupling constants could be deduced and compared to the theoretical values.

1. Introduction

The alkyl nitrates play an important role in tropospheric chemistry [1-4] and are also an important class of propellants and explosives [5, 6]. As such, *ab initio* and density functional theory calculations have been performed on a number of these compounds to determine their structures, as well as spectroscopic and thermodynamic properties [7-11]. Room temperature infrared spectra of the alkyl nitrates are not rotationally resolvable because of the high density of states introduced by the rotational isomerism of the alkyl chain and the modest barriers separating the conformers [11, 12]. Durig *et al.* were able to measure the torsional fundamental mode frequencies and barrier heights between the conformers for the two simplest alkyl nitrates, methyl and ethyl nitrate, in the far infrared range [13-15]. The microwave spectra of these molecules have been studied [16-18] and their structural parameters could be determined. True and Bohn measured low resolution microwave spectra of several other small chain alkyl nitrates [19]. Using relative intensity information at two sample temperatures (25 and −63 °C) and from estimated rotational constants of the conformers, they were able to assign the spectra to several conformers for each compound.

The microwave spectra of the two lowest energy conformers of *n*-propyl nitrate, $C_3H_7NO_3$, have been also reported [20]. The conformers are designated *anti-gauche* (*AG*) and *anti-anti* (*AA*), where these labels refer to the dihedral angles ∠(N-O-C1-C2) and ∠(O-C1-C2-C3) for each conformer, respectively. These spectra were measured using narrowband pulse excitation and broadband chirp excitation Fourier transform microwave (FTMW) spectroscopy, where the molecules were cooled in a supersonic expansion with argon as the carrier gas. To continue the series of this important class of compounds, we report here the spectra of five conformers of *n*-butyl nitrate, $C_4H_9NO_3$, measured using the same techniques, also under jet cooled conditions. The observed conformers are *AGA*, *AAA*, *GGA*, *GAA*, and *AGG* where the relevant dihedral angles are τ_2 = ∠(N-O-C1-C2), τ_3 = ∠(O-C1-C2-C3), and τ_4 = ∠(C1-C2-C3-C4). For atom numbering, see Figure 1. For the lowest energy *AGA* conformer, the spectra of the ^{15}N, ^{13}C(1), ^{13}C(2), ^{13}C(3), and ^{13}C(4) isotopologues were measured in natural abundance, assigned, and fitted. Therefore, select structural parameters for the *AGA* conformer could be determined, including two of the dihedral angles. The experimental values of spectroscopic and structural parameters are compared to those calculated by quantum chemistry.

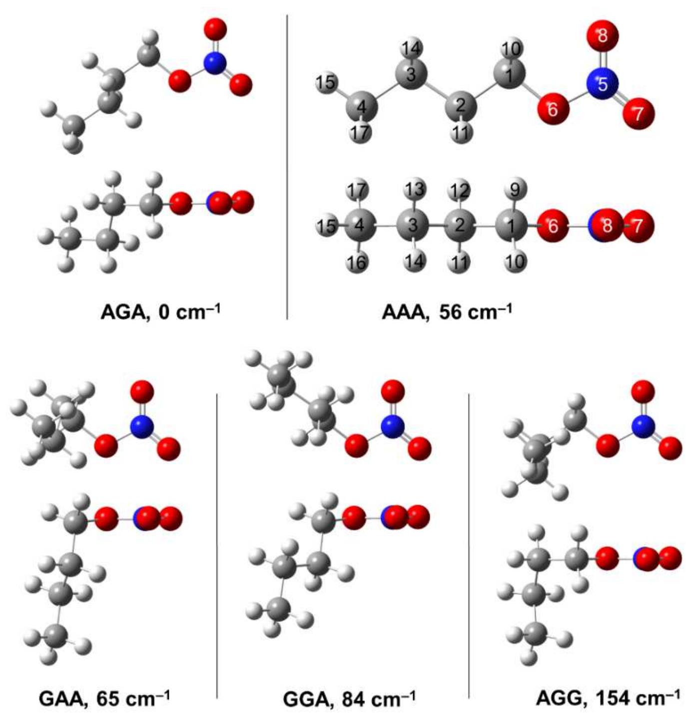

Figure 1. Molecular geometries of the five experimentally observed conformers of *n*-butyl nitrate optimized at the B2PLYP-D3/aug-cc-pVDZ level of theory. Upper trace for each conformer: structural view where the NO_3 group lies in the plane of the page; lower trace: structural view where the NO_3 group lies perpendicular to the plane of the page.

2. Methodology

2.1 Quantum Chemical Calculations

To predict the stable equilibrium structures of *n*-butyl nitrate and their energies, starting geometries were created by setting each of the three dihedral angles τ_2 = ∠(N-O-C1-C2), τ_3 = ∠(O-C1-C2-C3), and τ_4 = ∠(C1-C2-C3-C4) to 180°, ±120°, and 0°. There are thus four values to set for each dihedral angle, making a total of $4^3 = 64$ starting geometries, which were optimized at the B3LYP-D3/aug-cc-pVTZ level of theory using *GAUSSIAN* 16 [21]. Three starting geometries were eliminated due to strong steric hindrance. Varying the dihedral angle τ_1 = ∠(O-N-O-C1) results in configurations with a *gauche* nitrate group, which are known to not form local minima and are therefore eliminated from our conformational search by setting τ_1 = 0° for all starting geometries. Varying the dihedral angle τ_5 = ∠(C2-C3-C4-H) corresponds to the internal rotation of the methyl group at the end of the butyl chain, which does not create new conformers.

The conformational analysis resulted in the identification of thirteen stable conformers, which were confirmed as true local energy minima by harmonic frequency calculations, obtaining only real frequencies. These thirteen conformers were re-optimized at the B2PLYP-D3/aug-cc-pVDZ level. The B2PLYP method, developed by Zhang, Xu, and Goddard [22], performed well in optimizing conformers of *n*-propyl nitrate [20] while augmented with Grimme's dispersion corrections D3 [23]. The rotational constants, the dihedral angles τ_2, τ_3, τ_4, the dipole moment components, and energies relative to the most stable conformer I (*AGA*), are summarized in Table 1; the Cartesian coordinates can be found in Table S-1 in the Supplementary Material. As can be clearly recognized from Table 1, all thirteen conformers are within 5 $kJ\cdot mol^{-1}$ (ca. 420 cm^{-1}) of one another in energy. They all have C_1 point group symmetry, except conformer II (*AAA*) that features a straight butyl chain and belongs to the C_s point group. In the experimental spectrum, we eventually observed the five conformers lowest in energy, I (*AGA*), II (*AAA*), III (*GGA*), IV (*GAA*), and V (*AGG*). They are illustrated in Figure 1. Anharmonic frequency calculations were performed on these conformers to access the ground state rotational constants and quartic centrifugal distortion constants, which will be given below in comparison to the experimental values.

Table 1. Calculated rotational constants *A*, *B*, *C* (in MHz), dihedral angles τ_2, τ_3, τ_4 (in degree), dipole moment components μ_a, μ_b, μ_c (in Debye), conformer energies $E_{\mathrm{kJ\cdot mol}^{-1}}$ (in kJ·mol^{-1}) and $E_{\mathrm{cm}^{-1}}$ (in cm^{-1}) relative to $E_{\mathrm{AGA}} = -437.8033644$ Hartree of the thirteen conformers of *n*-butyl nitrate predicted at the B2PLYP-D3/aug-cc-pVDZ level of theory. The Boltzmann fractional populations are given for the thirteen conformers at a temperature of 296 K.

Conf.		***A***	***B***	***C***	τ_2	τ_3	τ_4	$\lvert\mu_a\rvert$	$\lvert\mu_b\rvert$	$\lvert\mu_c\rvert$	$E_{\mathrm{kJ\cdot mol}^{-1}}$	$E_{\mathrm{cm}^{-1}}$	**Pop.**
I	*AGA*	5581	848	777	179	66	179	3.17	1.57	0.11	0	0	18.9
II	*AAA*	7989	721	673	180	180	180	3.75	0.69	0.00	0.67	56	14.4
III	*GGA*	3917	1023	978	79	59	180	2.77	1.90	0.33	0.78	65	13.8
IV	*GAA*	5482	852	813	79	176	179	3.34	1.02	0.77	1.00	84	12.6
V	*AGG*	4112	1004	971	179	60	59	3.24	1.46	0.02	1.84	154	8.9
VI	*GGG*	4052	1134	1049	78	55	63	2.96	1.37	0.84	2.60	217	6.6
VII	*AAG*	5857	832	763	179	175	63	3.83	0.00	0.32	3.19	267	5.2
VIII	*GAG*	5095	965	888	80	173	65	3.48	0.75	0.56	3.74	313	4.1
IX	*GAG′*	6107	888	836	79	179	–63	3.59	0.21	0.44	3.81	318	4.0
X	*GG′A*	3524	1167	1033	95	–66	179	2.65	1.90	0.72	3.89	325	3.9
XI	*GGG′*	3191	1423	1198	75	59	–76	2.77	1.88	0.48	4.77	399	2.7
XII	*G′GG*	3287	1392	1163	–97	70	69	2.84	1.51	0.85	4.94	413	2.5
XIII	*AGG′*	3978	1109	942	180	76	–67	3.11	1.73	0.04	5.07	424	2.4

The nitrate group of *n*-butyl nitrate features a ^{14}N nucleus with a nuclear spin $I = 1$, resulting in hyperfine splittings of all rotational transitions observed in the microwave spectrum, which are characterized by the nuclear quadrupole coupling constants (NQCCs). To calculate the NQCCs, we used Bailey's semi-experimental method [24], where the electric field gradient (EFG) tensor of the ^{14}N nucleus was calculated at the B3PW91/6-311+G(df,pd) level on the molecular geometry optimized at the B2PLYP-D3/aug-cc-pVDZ level. The EFG tensor is directly proportional to the quadrupole coupling tensor by the calibration factor $eQ/h = -4.5586$ MHz/a.u. The results will also be given below in comparison to the experimental values.

2.2 Experimental

The microwave spectra of *n*-butyl nitrate were first measured with a broadband chirp excitation FTMW spectrometer. This instrument is based on the design by Pate and coworkers and has been described in detail elsewhere [25, 26]. The *n*-butyl nitrate sample was purchased from MP Biomedicals, LLC, and was used without further purification. A portion of the chirp excitation spectrum is shown in Figure 2.

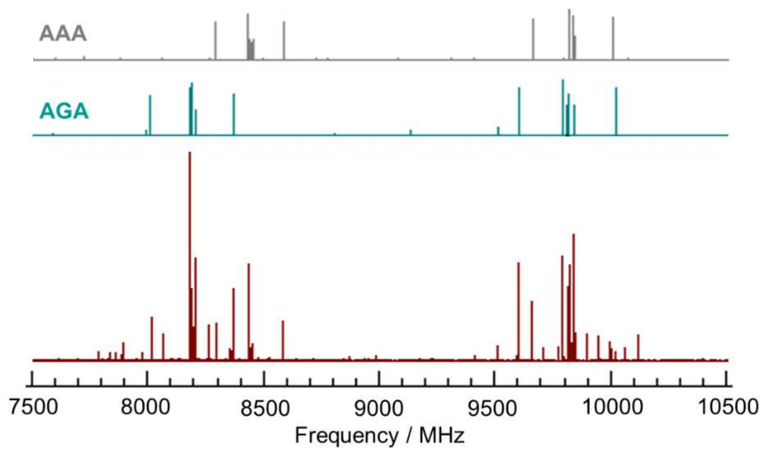

Figure 2. A portion of the chirp excitation FTMW spectrum of *n*-butyl nitrate from 7500 to 10500 MHz. The assigned transitions of the two most stable conformers *AGA* and *AAA* are given. The measurement accuracy is about 10 kHz.

All transitions for all conformers and isotopologues, after being identified from the chirp excitation spectrum, were remeasured with a narrowband pulse excitation FTMW spectrometer based on the design of Balle and Flygare because of its greater sensitivity and resolution [27-29]. Measurements were performed in the 5 to 20 GHz range. Briefly, a 1 mL sample of the volatile liquid sample (boiling point 133 °C; vapor pressure 8.3 Torr at 25 °C) was pipetted into a bubbler in the gas line leading to the gas pulse nozzle. Dry argon (99.999%, Airgas), with a backing pressure of 1.5 atm, was bubbled through the sample. This mixture was then expanded through the pulse nozzle into the Fabry-Perot type resonator of the spectrometer, placed in a chamber that was held under vacuum at 10^{-6} Torr. The molecules in the gas pulse undergo supersonic expansion, leaving them rotationally cold at 1-

2 K. Microwave radiation, lasting 0.9 µs, polarizes the sample concurrently undergoing supersonic expansion. After a delay of 26 µs following the radiation pulse, the free induction decay (FID) of the polarized sample is collected for 102.4 µs and digitized. Between a few hundred and a few thousand FIDs were co-added for each molecular transition, to improve the signal-to-noise ratio proportional to the square root of the number of co-added FIDs. The measured transitions have an average line width of 10 kHz with an uncertainty of ±1.5 kHz in the center frequency. They appear as Doppler doublets due to the coaxial arrangement of the molecular jet and the resonator. A typical Balle-Flygare high resolution spectrum is illustrated in Figure 3. The spectra of the various isotopologues were measured in natural abundance.

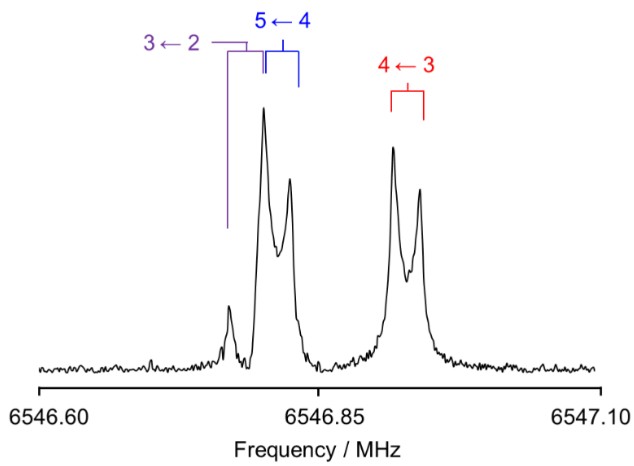

Figure 3. A typical high-resolution pulse excitation FTMW spectrum of the $4_{23} \leftarrow 3_{22}$ transition of the parent species of the *AGA* conformer. The ^{14}N nuclear quadrupole hyperfine splittings could be fully resolved and marked by $F' \leftarrow F$. Doppler doublets observed for all transitions are marked by brackets.

3. Results

3.1 Spectral Assignment and Fitting

We first started the spectral assignment with the most stable conformer I (*AGA*). Using the rotational constants predicted at the B2PLYP-D3/aug-cc-pVDZ level of theory, and with the estimates of the dipole moment components, spectral simulations for this conformer were performed using Pickett's *spcat* program [30, 31]. Microwave transitions of this conformer were quickly found using the Balle-Flygare resonator instrument. Strong *a*-type and weaker *b*-type transitions were observed, but no

c-type transitions, in agreement with the very small, predicted value of 0.11 D for the c-dipole moment component. The parameters of a Watson A-reduction Hamiltonian were fitted to the measured transition frequencies: [20, 30, 31]

$$\mathbf{H} = \mathbf{H}_R + \mathbf{H}_{CD} + \mathbf{H}_Q \tag{1}$$

where $\mathbf{H}_R$ and $\mathbf{H}_{CD}$ account for the rigid rotor and centrifugal (quartic) distortion energies, respectively. $\mathbf{H}_Q$ is the nuclear quadrupole coupling Hamiltonian, which is written as: [32-36]

$$\mathbf{H}_Q = \frac{1}{2I(2I-1)} \sum_{\alpha,\beta} \chi_{\alpha,\beta} \left[I_\alpha, I_\beta\right]_+ \tag{2}$$

and then, with some manipulation, can be rewritten in a form appropriate for use with Pickett's *spfit* program [30, 31]:

$$\begin{aligned}\mathbf{H}_Q = \frac{1}{2I(2I-1)} \Big\{ & \frac{3}{2}\chi_{aa}\left[I_a^2 - \frac{1}{3}\mathbf{I}^2\right] \\ & + \frac{1}{4}(\chi_{bb} - \chi_{cc})[I_+^2 + I_-^2] + \chi_{ab}[I_a I_b + I_b I_a] \\ & + \chi_{ac}[I_a I_c + I_c I_a] + \chi_{bc}[I_b I_c + I_c I_b] \Big\}\end{aligned} \tag{3}$$

where the χ_{ij} terms correspond to the components of the nuclear electric quadrupole coupling tensor. Note that none of the off-diagonal terms could be determined in the case of n-butyl nitrate due to the small quadrupole moment of the ^{14}N nucleus. Rotational transitions are labeled by quantum numbers of the form $J'_{K_a' K_c'} F' \leftarrow J_{K_a K_c} F$ where F is the total angular momentum quantum number that includes the nuclear spin and the rotational angular momentum of the molecule, $\boldsymbol{F} = \boldsymbol{I} + \boldsymbol{J}$. The spectroscopic constants resulting from the fit are summarized in Table 2. The quantum number assignments, measured transition frequencies, and observed-minus-calculated residuals are given in Table S-2 in the Supplementary Material.

Table 2. Molecular parameters of the parent species, as well as all ^{13}C isotopologues and the ^{15}N isotopologue of the *AGA* conformer of *n*-butyl nitrate obtained from least-squares fitting by *spfit*. Atoms are numbered according to Figure 1.

Par.[a]	Unit	^{12}C	$^{13}C(1)$	$^{13}C(2)$	$^{13}C(3)$	$^{13}C(4)$	^{15}N	Calc.[b]
A_0	MHz	5635.18815(46)	5574.8164(46)	5592.3022(83)	5616.24(55)	5617.3057(88)	5633.37(44)	5540
B_0	MHz	854.06500(27)	854.04835(46)	850.12164(39)	846.34689(49)	834.40201(57)	848.85592(46)	838
C_0	MHz	782.79094(26)	781.62751(48)	779.18725(41)	776.45431(52)	765.92014(56)	778.37753(38)	768
Δ_J	kHz	0.11140(53)	0.1102(31)	0.1102(22)	0.1107(45)	0.1068(42)	0.1095(22)	0.10253
Δ_{JK}	kHz	–1.9933(56)	–2.00(13)	–1.997(80)	–1.9933[c]	–1.98(26)	–2.02(29)	–1.84056
Δ_K	kHz	19.71703[d]	19.71703[d]	19.71703[d]	19.71703[d]	19.71703[d]	19.71703[d]	19.71703
δ_J	kHz	0.01349(30)	0.01349[c]	0.01349[c]	0.01349[c]	0.01349[c]	0.0132(15)	0.01290
δ_K	kHz	0.67(13)	0.6711[c]	0.6711[c]	0.6711[c]	0.6711[c]	0.6711[c]	0.51247
$1.5\chi_{aa}$	MHz	1.2870(14)	1.28697[c]	1.28697[c]	1.28697[c]	1.28697[c]		1.30220
$¼(\chi_{bb}–\chi_{cc})$[e]	MHz	–0.21476(56)	–0.21476[c]	–0.21476[c]	–0.21476[c]	–0.21476[c]		–0.17680
N[f]		89	40	45	27	27	19	
RMS[g]	kHz	0.7	0.8	1.2	2.2	0.8	0.2	

[a] All parameters refer to the principal axis system. Watson's A reduction and I^r representation were used.

[b] Ground state rotational constants and quartic centrifugal distortion constants from anharmonic frequency calculations at the B2PLYP-D3/aug-cc-pVDZ level of theory. NQCCs are obtained with Bailey's method using the B3PW91/6-311+G(df,pd)//B2PLYP-D3/aug-cc-pVDZ combination and the calibration factor eQ/h = –4.5586 MHz/a.u. [24].

[c] Fixed to the value of the parent species.

[d] Fixed to the calculated value.

[e] For the parent species, χ_{aa} = 0.85798 MHz, χ_{bb} = –0.85851 MHz, and χ_{cc} = 0.00053 MHz, derived from the fitted parameters $1.5\chi_{aa}$ and $¼(\chi_{bb} – \chi_{cc})$ and the Laplace relation $\chi_{aa} + \chi_{bb} + \chi_{cc} = 0$.

[f] Number of lines.

[g] Root-mean-square deviation of the fit.

We then searched for the (*AGA*) ^{13}C isotopologues in natural abundance using the Balle-Flygare spectrometer due to its high sensitivity and could observe the spectra of all four ^{13}C species in natural abundance (1.1%), including the hyperfine structures arising from the I = 1 nuclear spin of the ^{14}N nucleus. The microwave spectrum of the ^{15}N isotopologue, with a natural abundance of 0.8%, could also be detected. ^{15}N has I = ½ nuclear spin and does not give rise to hyperfine splittings. The molecular parameters resulting from the least-squares fitting are given in Table 2 along with those of the parent species. The frequency lists together with the observed-minus-calculated residuals are also available in Table S-2 in the Supplementary Material. Searches for transitions from the ^{18}O isotopologues were unsuccessful. No transitions from D isotopologues were observed.

We then searched for the other conformers of *n*-butyl nitrate in the chirp excitation spectrum and found transitions for the *AAA*, *GGA*, *GAA*, and *AGG* conformers. Transitions for these conformers were subsequently remeasured using the Balle-Flygare resonator instrument to determine the frequencies with higher precision. The fit results for these conformers are given in Table 3. The transition frequencies are reported in Table S-3 in the Supplementary Material. We could not confidently assign any other conformers. No splittings were observed due to internal rotation of the terminal methyl group on the alkyl chain.

Table 3. Molecular parameters of the *AAA*, *GGA*, *GAA*, and *AGG* conformers of *n*-butyl nitrate obtained from least-squares fitting by *spfit*.

Par.[a]	**Unit**	***AAA* (II)**	**Calc.**[b]	***GGA* (III)**	**Calc.**[b]	***GAA* (IV)**	**Calc.**[b]	***AGG* (V)**	**Calc.**[b]
A_0	MHz	8043.3670(49)	7898	4012.1(19)	3513	5566.1066(22)	5452	4226.6(12)	3920
B_0	MHz	727.06170(30)	714	1017.4609(12)	1140	853.81046(42)	840	991.29978(88)	1003
C_0	MHz	678.50328(31)	666	974.8536(11)	1014	816.02864(40)	802	964.61878(72)	961
Δ_J	kHz	0.01717(78)	0.01640	0.5654(75)	0.4612	0.1431(25)	0.1303	0.5820(26)	0.5393
Δ_{JK}	kHz	0.220(33)	0.2250	–5.36(83)	–2.4226	–2.502(58)	–2.2389	–3.693(93)	–5.0085
Δ_K	kHz	3.4012[c]	3.4012	8.2443[c]	8.2443	26.2848[c]	26.2848	19.1948[c]	19.1948
δ_J	kHz	0.001183[c]	0.001183	0.0839(53)	0.0914	0.0133(26)	0.01201	0.0659(34)	0.0876
δ_K	kHz	0.03165[c]	0.03165	–0.3386[c]	–0.3386	0.8772[c]	0.8772	0.8146[c]	0.8146
$1.5\chi_{aa}$	MHz	0.876(16)		0.2817[c]		–0.300(20)		1.061(71)	
χ_{aa}[d]	MHz	0.584(11)[d]	0.5990		0.1878	–0.200(14)[d]	–0.2195	0.707(48)[d]	0.7239
$¼(\chi_{bb}–\chi_{cc})$	MHz	–0.1482(77)		0.0594[c]		0.1900(50)		–0.122(24)	
χ_{bb}[d]	MHz	–0.588(21)	–0.5080		–0.2127	0.480(17)	0.4573	–0.597(71)	–0.5580
χ_{cc}[d]	MHz	0.00	–0.0910		0.0249	–0.280(37)	–0.2378	–0.11(17)	–0.1660
N[e]		54		21		66		45	
RMS[f]	kHz	0.5		3.5		0.7		3.5	

[a] All parameters refer to the principal axis system. Watson's A reduction and I^r representation were used.
[b] Ground state rotational constants and quartic centrifugal distortion constants from anharmonic frequency calculations at the B2PLYP-D3/aug-cc-pVDZ level of theory. NQCCs are obtained with Bailey's method using the B3PW91/6-311+G(df,pd)//B2PLYP-D3/aug-cc-pVDZ combination and the calibration factor eQ/h = –4.5586 MHz/a.u. [24].
[c] Fixed to the calculated value.
[d] Derived from the fitted parameter $1.5\chi_{aa}$ and $0.25(\chi_{bb} – \chi_{cc})$ and the Laplace relation $\chi_{aa} + \chi_{bb} + \chi_{cc} = 0$.
[e] Number of lines.
[f] Root-mean-square deviation of the fit.

3.2 Structure Determination of the AGA Conformer

For the most stable *AGA* conformer, we could measure, in natural abundance, six sets of rotational constants: the parent species, four ^{13}C isotopologues, and the ^{15}N isotopologue. The available information allowed us to determine the heavy atom substitution structure r_s using Kraitchman's equations [37] as implemented in the programs *KRA* and *EVAL* [38]. The signs of the atom coordinates were taken from the optimized geometry r_e given in Table 4 and Table S-1 of the Supplementary Material and the uncertainties were calculated with Costain's rule [39]. The experimentally determined atom coordinates are also reported in Table 4, the bond angles and bond lengths in Table 5. The *a*-coordinate of the C(1) atom and the *c*-coordinate of the nitrogen atom are small and their uncertainties are larger than the determined values. Therefore, we set these coordinates to zero; i.e., the C(1) atom lies in the *bc* inertia plane and the nitrogen atom in the *ab* plane.

Table 4. The r_s atom positions of the most stable *AGA* conformer of *n*-butyl nitrate obtained from isotopic substitutions with Kraitchman's equations [37] as implemented in the program KRA [38], as well as the r_0 atom positions obtained with the program *STRFIT* [40]. Atom positions from the r_e geometry optimized at the B2PLYP-D3/aug-cc-PVDZ level of theory are also given.

	r_e			r_0			r_s		
	a / Å	b / Å	c / Å	a / Å	b / Å	c / Å	a / Å	b / Å	c / Å
C(1)	0.161448	–0.988979	–0.113111	0.1550(84)	–0.9774(24)	–0.1187(90)	0.0	–0.9823(15)	–0.106(15)
C(2)	1.606465	–0.690831	–0.478402	1.5973(25)	–0.6760(41)	–0.4808(87)	1.59087(95)	–0.6835(22)	–0.4769(32)
C(3)	2.292859	0.297586	0.469454	2.2854(18)	0.293(10)	0.4676(90)	2.2813(12)	0.2977(91)	0.4674(58)
C(4)	3.754567	0.542654	0.088273	3.7445(10)	0.5328(53)	0.0917(74)	3.74197(40)	0.5387(29)	0.069(22)
N(5)	–1.931683	0.181346	0.029432	–1.9213(12)	0.1791(10)	0.0302(11)	–1.9164(13)	0.172(14)	0.0
O(6)	–0.556475	0.265980	–0.292477	–0.5580(76)	0.2650(83)	–0.2928(80)			
O(7)	–2.515695	1.231545	–0.122367	–2.5069(56)	1.2288(42)	–0.1186(25)			
O(8)	–2.356079	–0.896796	0.407597	–2.3434(64)	–0.9001(48)	0.4082(76)			

Table 5. Bond lengths, bond angles, and dihedral angles deduced from the r_e, r_s and r_0 structures of the most stable *AGA* conformer of *n*-butyl nitrate.

	r_e	r_0	r_s
		Bonds lengths / Å	
C1–C2	1.52000	1.5173(63)	1.6608(35)
C2–C3	1.53184	1.5202(91)	1.5268(73)
C3–C4	1.53034	1.5257(58)	1.5331(62)
		Bond angles / °	
C4–C3–C2	112.15999	112.30(74)	111.78(75)
C3–C2–C1	113.81851	114.08(73)	114.24(44)
		Dihedral angles / °	
C4–C3–C2–C1	178.53257	178.20(81)	179.66(67)
C3–C2–C1–N5	64.44932	65.84(87)	63.4(12)

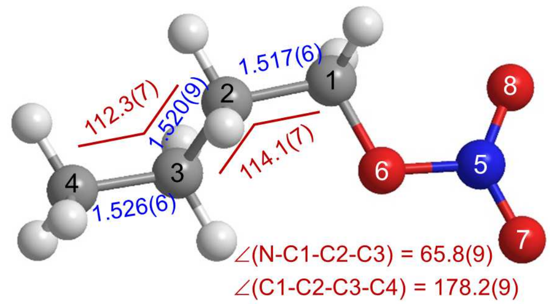

Figure 4. Bond lengths (blue, in Å), bond angles and dihedral angles (dark red, in degrees) of the r_0 structure of the *AGA* conformer of *n*-butyl nitrate.

Since only the microwave spectra of the ^{13}C and ^{15}N isotopologues could be observed, no information on the locations of the oxygen and the hydrogen atoms is available, making a complete structure determination impossible. However, the coordinates of the oxygen and the hydrogen atoms can be taken from the r_e structure calculated at the B2PLYP-D3/aug-cc-pVDZ level and least-squares fitted with the experimental rotational constants obtained using the program *STRFIT* [40]. The program varies the internal coordinates to obtain a minimum value of the squared deviations of all moments of inertia summed over all isotopologues where experimental values are available. This r_0 structure is also shown in Tables 4 and 5 and visualized in Figure 4. The *STRFIT* output summary is given in Table S-4 in the Supplementary Material.

4. Discussion

In our previous study on *n*-propyl nitrate, only two conformers were observed: the *anti-gauche AG* and *anti-anti AA* conformers. The other two conformers, *GA* and *GG´*, that should be local energy minima were not observed [20]. No far-infrared studies are available and no CH_3 torsional splittings were observed. In a 1983 low-resolution microwave study, True and Bohn [19] identified four *a*-type *R*-branches of *n*-butyl nitrate in the 20-25 GHz range. Their spectra, which were observed both at ~ −63°C and 22°C, allowed determination of $B + C$ values and compared these to estimates of $B + C$ based on the expected dihedral angles of 180 and 60°. In their 1983 study, only the *AAA* conformer was confidently assigned with a $B + C$ value of 1408.7(5) MHz; our value for this conformer is 1405.56498(61) MHz (see Table 3). True and Bohn identified a conformer with a $B + C$ value of 1644(3)

MHz that they labeled as "C." Our *AGA* conformer $B + C$ value is 1636.85594(53) MHz (see Table 2). They identified a third conformer with a $B + C$ value of 1671(2) MHz, which is close to our *GAA* experimental $B + C$ value of 1669.83910(82) MHz. They observed a fourth conformer that they labeled as "B" with a $B + C$ value of 1604.4(5) MHz. This value is not close to any of our experimental or calculated $B + C$ values. The conformer B was observed to have a slightly weaker microwave absorption intensity. Therefore, it may be from a vibrational hot band. In addition to the three conformers reported by True and Bohn, we observed two additional conformers, *GGA* ($B + C$ = 1992 MHz) and *AGG* ($B + C$ = 1956 MHz). The spectra of these are relatively strong compared to the slightly more abundant *AAA* conformer owing to their *gauche* structures that give larger dipole moments along the *b* and *c* rotational axes, and therefore more transitions to observe and fit in their microwave spectra.

The agreement between the calculated and the experimental rotational constants is not satisfactory for the assigned conformers. Therefore, the structure determination from the ^{13}C and ^{15}N isotopologues observed for conformer *AGA* is very useful because it confirms that the most stable conformer of *n*-butyl nitrate has a non-straight butyl chain. The γ-carbon atom (counting from the oxygen atom, C(3) in Figures 1 and 4) is out of the NO_3 plane and the dihedral angle ∠(C3-C2-C1-N) is around 64°. This corresponds well to the value of 65.2(9)° reported for the *AG* conformer of *n*-propyl nitrate. The ∠(C4-C3-C2-C1) dihedral angle is almost exactly 180°, showing that after being tilted out at the γ-carbon position, the alkyl chain continues being straight. This is quite often observed for short alkyl chains in other classes of compounds, such as in ketones (hexan-2-one [41]) and esters (*n*-butyl acetate [42] and ethyl butyrate [43]).

Examining the calculated dihedral angles for *n*-butyl nitrate given in Table 1, we see that the *AAA* conformer should have a planar heavy atom structure. Though a structure determination is not possible due to the lack of microwave data from its minor isotopologues, we can check the planarity by calculating the second moment $P_{cc} = (I_a + I_b - I_c)/2$. Buschmann et al. have noted that for small, rigid molecules each CH_2/CH_3 group contributes about 1.6 uÅ^2 to the second moment [44]. This assumes the nitrate group is planar. For the *AAA* conformer of *n*-butyl nitrate, there are four CH_2/CH_3 groups, corresponding to $4 \times 1.6 = 6.4$ uÅ^2. This is close to the value of 6.543 uÅ^2 calculated from the observed rotational constants and is consistent with heavy atoms of the *AAA* conformer lying in the *ab*-plane. A similar analysis was performed on the *AA* conformer of *n*-propyl nitrate [20]. This confirms that the conformer with the rotational constants A = 8043.3670(49) MHz, B = 727.06170(30) MHz, and C = 678.50328(31) MHz is the *AAA* conformer.

The assignment of a set of experimental microwave constants to a particular calculated conformer structure is much less obvious, particularly for the three conformers with weaker spectra. By comparing the experimental B_0^ξ (with $\xi = a, b, c$) and the calculated B_e^ξ rotational constants, as well as considering the energies of the conformers, we came to the conclusion that they are the conformers *GAA*, *GGA*, and *AGG* (see Table 6). Note that the calculated B_e^ξ constants from geometry optimizations shown in Table 1 are closer to the experimental B_0^ξ constants than the calculated B_0^ξ constants obtained from anharmonic frequency calculations shown in Table 3 due to error compensations. Using a simple Boltzmann analysis, we calculated the fractional population, at 296 K, of the *AGA*, *AAA*, *GAA*, *GGA*, and *AGG* to be 18.9%, 14.4%, 12.6%, 13.8%, and 8.9%, respectively, as given in the last column of Table 1. They are the five most stable conformers, and it is not surprising that they could all be observed. Since it is possible that the *AGG* conformer relaxes into the most stable *AGA* conformer during the supersonic expansion, as observed for ethyl butyrate [43], we calculated a potential energy curve containing the conversion of *AGG* to *AGA* by changing the dihedral angle $\tau_4 = \angle$(C1-C2-C3-C4) in 10° steps, as shown in Figure 5. The energy required to convert conformer *AGG* to conformer *AGA* is 10.76 kJ·mol^{-1} (899.5 cm^{-1}). This is a high barrier to overcome, and therefore *AGG* should remain populated in the jet-cooled spectra of *n*-butyl nitrate. We note that there are still unassigned lines remaining in the chirp excitation spectrum. It is thus possible that also other higher energy conformers are present, but we could not achieve a confident assignment for any of them.

Table 6. Experimental (Expt.) and B2PLYP-D3/aug-cc-pVDZ calculated (Calc.) rotational constants A, B, and C (in MHz) of the five observed conformers of *n*-butyl nitrate. The differences between the calculated and the experimental values (in MHz) are given as ΔA, ΔB, and ΔC.

Conf.	A	ΔA	B	ΔB	C	ΔC
AGA Calc.	5581.1		848.1		776.7	
AGA Expt.	5635.2	54.1	854.1	6.0	782.8	6.1
AAA Calc.	7988.5		721.2		673.7	
AAA Expt.	8043.4	54.9	727.1	5.9	678.5	4.8
GGA Calc.	3916.9		1022.6		978.4	
GGA Expt.	4012.1	95.2	1017.5	–5.1	974.9	–3.5
GAA Calc.	5482.4		852.0		813.0	
GAA Expt.	5566.1	83.7	853.8	1.8	816.0	3.0
AGG Calc.	4112.5		1004.3		971.5	
AGG Expt.	4226.6	114.1	991.3	–13.0	964.6	–6.9

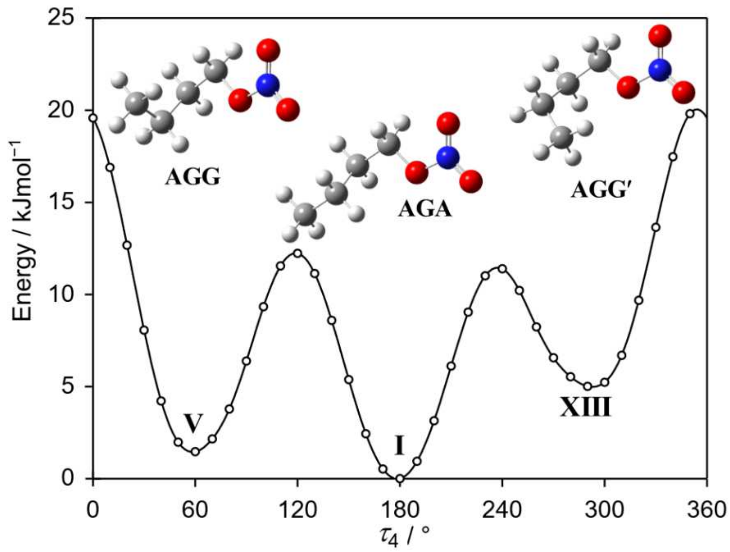

Figure 5. The potential energy curve of *n*-butyl nitrate obtained by varying the dihedral angle $\tau_4 = \angle$(C1-C2-C3-C4) in a 10°-grid. All other geometry parameters were optimized at the B2PLYP-D3/aug-cc-pVDZ level of theory. Energies relative to the lowest energy conformations are given. The potential curve captures conformer *AGA* (I, observed), *AGG* (V, observed), and *AGG′*(XIII, not observed).

Concerning the NQCCs, a direct comparison between the differently oriented conformers as well as with the *AG* and *AA* conformers of *n*-propyl nitrate is not possible because of the different principal axis systems. However, we can directly compare the χ_{cc} values of the *AAA* conformer of *n*-butyl nitrate and the *AA* conformer of *n*-propyl nitrate since they both possess an *ab*-symmetry plane.

Therefore, one principal axis of the nitrogen coupling tensor is collinear with the *c*-principal axis. We find a value of almost zero in both cases. Note that the same situation is observed for the *AGA* conformer of *n*-butyl nitrate and the *AG* conformer of *n*-propyl nitrate, though the values could not be directly compared. Our intuitive explanation is that for these conformers, the electronic wavefunction environment of the nitrogen nucleus is very symmetric within the *ab*-plane of the molecule.

5. Conclusions

We identified the five most stable conformers of *n*-butyl nitrate under molecular jet conditions using broadband chirp as well as narrowband pulse excitation FTMW spectroscopic techniques. The r_s and r_0 structures of the most stable conformer, *AGA*, could be determined from the observation of all ^{13}C and the ^{14}N isotopologue spectra, confirming that the *n*-butyl group is not straight, but tilted out from the NO_3 plane at the γ-carbon atom position by about 64°. The second conformer, *AAA*, features a C_s symmetry where all heavy atoms lay on the *ab*-plane and the χ_{cc} value of the nuclear quadrupole coupling tensor is zero. The identification of other conformers was based on comparison of the experimental fit constants with the calculated rotational constants as well as the relative energies.

Declaration of Competing Interests

The authors declare that they have no known competing financial interests or personal relationships that could have appeared to influence the work reported in this paper.

CRediT Authorship Contribution Statement

Susanna L. Stephens: Investigation, Data curation, Formal analysis, Writing - Original Draft preparation. **Eléonore Antonelli:** Investigation, Formal analysis, Visualization, Writing-Review & Editing. **Alexander B. Seys**: Investigation, Writing-Review & Editing. **Ha Vinh Lam Nguyen**: Investigation, Formal analysis, Visualization, Validation, Writing - Original Draft preparation, Supervision, Resources. **Stewart E. Novick**: Investigation, Writing-Review & Editing, Supervision, Resources. **S. A. Cooke:** Investigation, Writing-Review & Editing, Resources. **Thomas A. Blake**: Conceptualization, Investigation, Formal analysis, Validation, Writing - Original Draft preparation.

Acknowledgements

We thank J.A. Signore for performing some measurements and the National Science Foundation for financial support, Grant Number CHE – 1565276. S.A.C. also thanks Purchase College for support via the Taina Chao Fellowship. T.A.B. would like to thank Dr. Brienne Seiner of the Pacific Northwest National Laboratory for her interest in this work. The Pacific Northwest National Laboratory is operated by Battelle Memorial Institute for the U.S. Department of Energy under Contract No. DE-AC05-76RL01830. H.V.L.N. and E.A. were supported by the European Union (ERC 101040480-LACRIDO). Views and opinions expressed are, however, those of the authors only and do not necessarily reflect those of the European Union or the European Research Council. Neither the European Union nor the granting authority can be held responsible for them.

References

1. J. M. Roberts, The atmospheric chemistry of organic nitrates, Atmos. Environ. 24a (1990) 243-287. https://doi.org/10.1016/0960-1686(90)90108-Y

2. M. P. Turberg, D. M. Giolando, C. Tilt, T. Soper, S. Mason, M. Davies, P. Klingensmith, G. A. Takacs, Atmospheric photochemistry of alkyl nitrates, J. Photochem. Photobio. 51a (1990) 281-292. https://doi.org/10.1016/1010-6030(90)87063-h

3. J. N. Cape, S. E. Cornell, T. D. Jickells, E. Nemitz, Organic nitrogen in the atmosphere – Where does it come from? A Review of sources and methods, Atmos. Res. 102 (2011) 30-48. https://doi.org/10.1016/j.atmosres.2011.07.009

4. B. J. Finlayson-Pitts, J. N. Pitts, Jr., *Chemistry of the Upper and Lower Atmosphere*, Academic Press, New York, 1999. https://doi.org/10.1016/B978-0-12-257060-5.X5000-X

5. R. Boschan, R. T. Merrow, R. W. van Dolah, The chemistry of nitrate esters, Chem. Rev. 55 (1955) 485-510. https://doi.org/10.1021/cr50003a001

6. M. Marshall, J. C. Oxley (Eds.) *Aspects of Explosives Detection*, Elsevier, Amsterdam, Netherlands, 2009; see Chapter 2, Explosives: The Threat and Materials by M. Marshall, J. C. Oxley.

7. X. Gong, H. Xiao, B. van de Graaf, Ab initio studies on four alkyl nitric esters, J. Mol. Struct. 393 (1997) 207-212. https://doi.org/10.1016/S0166-1280(96)04860-9

8. X. D. Gong, H. M. Xial, Ab initio and density functional methods studies on the conformations and thermodynamic properties of propyl nitrate, J. Mol. Struct. 498 (2000) 181-190. https://doi.org/10.1016/S0166-1280(99)00259-6

9. X. D. Gong, H. M. Xial, Studies on the molecular structures, vibrational spectra and thermodynamic properties of organic nitrates using density functional theory and ab initio methods, J. Mol. Struct. 572 (2001) 213-221. https://doi.org/10.1016/S0166-1280(01)00633-9

10. X.-L. Zeng, W.-H. Chen, J.-C. Liu, J.-L. Kan, A theoretical study of five nitrates: Electronic structure and bond dissociation energies, J. Mol. Struct. 810 (2007) 47-51. https://doi.org/10.1016/j.theochem.2007.01.040

11. R. M. Shaikhullina, G. M. Hrapkovsky, M. M/ Shaikhullina, *N*-propyl nitrate vibrational spectrum analysis using DFT B3LYP quantum-chemical method, J. Phys.: Conf. Series 1015 (2018) 032125. https://doi.org/10.1088/1742-6596/1015/3/032125

12. J. C. D. Brand. T. M. Cawthon, The vibrational spectrum of methyl nitrate, J. Am. Chem. Soc. 77 (1955) 319-323. https://doi.org/10.1021/ja01607a019

13. B. J. van der Veken, G. A. Guirgis, J. R. Durig, Far-infrared spectra of methyl nitrate and methyl-d_3 nitrate, J. Mol. Struct. 142 (1986) 105-110. https://doi.org/10.1016/0022-2860(86)85073-6

14. J. R. Durig, N. E. Lindsay, Far-infrared spectra and barriers to internal rotation of ethyl nitrate, Spectrochimica Acta A 46 (1990) 1125-1135. https://doi.org/10.1016/0584-8539(90)80230-V

15. J. R. Durig, T. G. Sheehan, Raman spectra, vibrational assignment, structural parameters and ab initio calculations for ethyl nitrate, J. Raman Spectrosc. 21 (1990) 635-644. https://doi.org/10.1002/jrs.1250211003

16. W. B. Dixon, E. B. Wilson, Jr., Microwave spectrum of methyl nitrate, J. Chem. Phys. 35 (1961) 191-198. https://doi.org/10.1063/1.1731890

17. A. P. Cox, S. Waring, Microwave spectrum, structure and dipole moment of methyl nitrate, Trans. Faraday Soc. 67 (1971) 3441-3450. https://doi.org/10.1039/TF9716703441

18. D. G. Scroggin, J. M. Riveros, E. B. Wilson, Microwave spectrum and rotational isomerism of ethyl nitrate, J. Chem. Phys. 60 (1974) 1376-1385. https://doi.org/10.1063/1.1681207

19. N. S. True, R. K. Bohn, Low resolution microwave spectra and conformations of five nitric acid esters, Spectrochimica Acta A 39 (1983) 867-875. https://doi.org/10.1016/0584-8539(83)80167-6

20. W. Orellana, S. L. Stephens, S. E. Novick, S. A. Cooke, C. S. Brauer, T. A. Blake, A study of the conformational isomerism of *n*-propyl nitrate by microwave spectroscopy. J. Mol. Spectrosc. 374 (2020) 111376. https://doi.org/10.1016/j.jms.2020.111376

21. M. J. Frisch, G. W. Trucks, H. B. Schlegel, G. E. Scuseria, M. A. Robb, J. R. Cheeseman, G. Scalmani, V. Barone, G. A. Petersson, H. Nakatsuji, X. Li, M. Caricato, A. V. Marenich, J. Bloino, B. G. Janesko, R. Gomperts, B. Mennucci, H. P. Hratchian, J. V. Ortiz, A. F. Izmaylov, J. L. Sonnenberg, D. Williams-Young, F. Ding, F. Lipparini, F. Egidi, J. Goings, B. Peng, A. Petrone, T. Henderson, D. Ranasinghe, V. G. Zakrzewski, J. Gao, N. Rega, G. Zheng, W. Liang, M. Hada, M. Ehara, K. Toyota, R. Fukuda, J. Hasegawa, M. Ishida, T. Nakajima, Y. Honda, O. Kitao, H. Nakai, T. Vreven, K. Throssell, J. A. Montgomery, Jr., J. E. Peralta, F. Ogliaro, M. J. Bearpark, J. J. Heyd, E. N. Brothers, K. N. Kudin, V. N. Staroverov, T. A. Keith, R. Kobayashi, J. Normand, K. Raghavachari, A. P. Rendell, J. C. Burant, S. S.

Iyengar, J. Tomasi, M. Cossi, J. M. Millam, M. Klene, C. Adamo, R. Cammi, J. W. Ochterski, R. L. Martin, K. Morokuma, O. Farkas, J. B. Foresman, D. J. Fox, Gaussian 16, Revision B.01, Inc., Wallingford CT, 2016.

22. Y. Zhang, X. Xu, W.A. Goddard III, Double hybrid density functional for accurate descriptions of nonbond interactions, thermochemistry and thermochemical kinetics, Proc. Nat. Acad. Sci. 106 (2009) 4963-4968. https://doi.org/10.1073/pnas.0901093106

23. S. Grimme, M. Steinmetz, Effects of London dispersion correction in density functional theory on the structures of organic molecules in the gas phase, Phys. Chem. Chem. Phys. 15 (2013) 16031-16042. https://doi.org/10.1039/C3CP52293H

24. W.C. Bailey, DFT and HF–DFT calculations of ^{14}N quadrupole coupling constants in molecules, Chem. Phys. 252 (2000) 57-66, doi:10.1016/S0301-0104(99)00342-0

25. G. G. Brown, B. C. Dian, K. O. Douglass, S. M. Geyer, S. T. Shipman, B. H. Pate, A broadband Fourier transform microwave spectrometer based on chirped pulse excitation, Rev. Sci. Instrum. 79 (2008) 053103. https://doi.org/10.1063/1.2919120

26. G. S. Grubbs II, C. T. Dewberry, K. C. Etchison, K. E. Kerr, S. A. Cooke, A search accelerated correct intensity Fourier transform microwave spectrometer with pulsed laser ablation source, Rev. Sci. Instrum. 78 (2007) 096106. https://doi.org/10.1063/1.2786022

27. T. Balle, W. Flygare, Fabrey-Perot cavity pulsed Fourier transform microwave spectrometer with a pulsed nozzle particle source, Rev. Sci. Instrum. 52 (1981) 33-45. https://doi.org/10.1063/1.1136443

28. G. S. Grubbs II, D. A. Obenchain, H. M. Pickett, S. E. Novick, H_2-AgCl: A spectroscopic study of a dihydrogen complex, J. Chem. Phys. 141 (2014) 114306. https://doi.org/10.1063/1.4895904

29. A. H. Walker, W. Chen, S. E. Novick, B. D. Bean, M. D. Marshall, Determination of the structure of HBr OCS, J. Chem. Phys. 102 (1995) 7298-7305. https://doi.org/10.1063/1.469041

30. H. M. Pickett, The fitting and prediction of vibration-rotation spectra with spin interactions, J. Mol. Spectrosc. 148 (1991) 371-377. https://doi.org/10.1016/0022-2852(91)90393-O

31. S. E. Novick, A beginner's guide to Pickett's SPCAT/SPFIT, J. Mol. Spectrosc. 329 (2016) 1-7. https://doi.org/10.1016/j.jms.2016.08.015

32. D. Posener, Coupling of nuclear spins in molecules, Aust. J. Phys. 11 (1958) 1−17. http://dx.doi.org/10.1071/ph580001

33. P. Thaddeus, L. Krisher, J. Loubser, Hyperfine structure in the microwave spectrum of HDO, HDS, CH_2O, and CHDO: beam-maser spectroscopy on asymmetric-top molecules, J. Chem. Phys. 40 (1964) 257−273. https://doi.org/10.1063/1.1725107

34. D. Boucher, J. Burie, D. Dangoisse, J. Demaison, A. Dubrulle, Doppler-free rotational spectrum of methyl iodide. Nuclear quadrupole, spin-rotation and nuclear shielding tensors of iodine, Chem. Phys. 29 (1978) 323−330. https://doi.org/10.1016/0301-0104(78)85082-4

35. E. Hirota, J. M. Brown, J. Hougen, T. Shida, N. Hirota, Symbols for fine and hyperfine structure parameters (IUPAC Recommendations 1994), Pure Appl. Chem. 66 (1994) 571−576. https://doi.org/10.1351/pac199466030571

36. E. A. Arsenault, D. A. Obenchain, Y. J. Choi, T. A. Blake, S. A. Cooke, S. E. Novick, A study of 2-iodobutane by rotational spectroscopy, J. Phys. Chem. A 120 (2016) 7145-7151. https://doi.org/10.1021/acs.jpca.6b06938

37. J. Kraitchman, Determination of molecular structure from microwave spectroscopic data, Am. J. Phys. 21 (1953) 17−24. https://doi.org/10.1119/1.1933338

38. Z. Kisiel, PROSPE-Programs for ROtational SPEctroscopy, available at http://info.ifpan.edu.pl/~kisiel/prospe.htm.

39. C. C. Costain, Further comments on the accuracy of r_s substitution structures, Trans. Am. Crystallogr. Assoc. 2 (1966) 157-164.

40. Z. Kisiel, Least-squares mass-dependence molecular structures for selected weakly bound intermolecular clusters. J. Mol. Spectrosc. 218 (2003) 58−67. https://doi.org/10.1016/S0022-2852(02)00036-X

41. M. Andresen, I. Kleiner, M. Schwell, W. Stahl, H. V. L. Nguyen, Sensing the molecular structures of hexan-2-one by internal rotation and microwave spectroscopy, ChemPhysChem 20 (2019) 2063–2073. https://doi.org/10.1002/cphc.201900400

42. T. Attig, L. W. Sutikdja, R. Kannengießer, I. Kleiner, W. Stahl, The microwave spectrum of *n*-butyl acetate, J. Mol. Spectrosc. 284-285 (2013) 8-15. https://doi.org/10.1016/j.jms.2013.02.003

43. L.W. Sutikdja, H. V. L. Nguyen, D. Jelisavac, W. Stahl, H. Mouhib, Benchmarking quantum chemical methods for accurate gas-phase structure predictions of carbonyl compounds: the case of ethyl butyrate, Phys. Chem. Chem. Phys. 25 (2023) 7688–7696. https://doi.org/10.1039/d2cp05774c.

44. P. Buschmann, K. G. Lengsfeld, J. Djahandideh, J.-U. Grabow, From rotational resolved spectra to an extended increment system of planar moments allowing ad-hoc conformational identification – Exemplification by the broadband microwave spectrum of α-hydroxyisobutyric acid, J. Mol. Struct. 1250 (2022) 131805. https://doi.org/10.1016/j.molstruc.2021.131805